Linear Stability of the Rotating Disk Boundary Layer

Scott Morgan

Supervisor: Dr. Chris Davies

- Why study rotating disks?

- Why study rotating disks?
- Why study oscillatory motion on the disk?

Introduction to the Rotating Disk - Setup

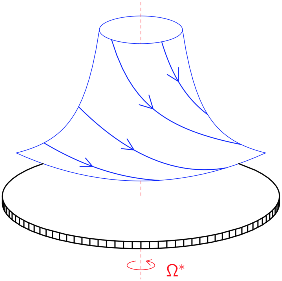

Figure 1: Rotating Disk Profile

Introduction to the Rotating Disk - History

- Why is it an interesting problem?
  - Canonical example of a three-dimensional boundary layer.

Introduction to the Rotating Disk - History

- Why is it an interesting problem?
  - Canonical example of a three-dimensional boundary layer.
  - Approximation to swept-wing flow.

Introduction to the Rotating Disk - History

- Why is it an interesting problem?
  - Canonical example of a three-dimensional boundary layer.
  - Approximation to swept-wing flow.
  - More amenable to experiments.

Introduction to the Rotating Disk - Setup

- First studied in 1921 by Theodore von Kármán who derived an exact similarity solution to the Navier Stokes equations.

$$F(z) = \frac{U^*}{r^*\Omega^*}, \quad G(z) = \frac{V^*}{r^*\Omega^*}, \quad H(z) = \frac{W^*}{(\nu\Omega^*)^{\frac{1}{2}}}$$

where $\mathbf{U} = \mathbf{U}^*(z)$ is the velocity profile in cylindrical polars, Ω^* is the rotation rate of the disk and ν is the kinematic viscosity.

Introduction to the Rotating Disk - Setup

- First studied in 1921 by Theodore von Kármán who derived an exact similarity solution to the Navier Stokes equations.

$$F(z) = \frac{U^*}{r^*\Omega^*}, \quad G(z) = \frac{V^*}{r^*\Omega^*}, \quad H(z) = \frac{W^*}{(\nu\Omega^*)^{\frac{1}{2}}}$$

  where $\mathbf{U} = \mathbf{U}^*(z)$ is the velocity profile in cylindrical polars, Ω^* is the rotation rate of the disk and ν is the kinematic viscosity.

- Worth noting - Reynolds number is equivalent to radial position on the disk.

Introduction to the Rotating Disk - Setup

- First studied in 1921 by Theodore von Kármán who derived an exact similarity solution to the Navier Stokes equations.

$$F(z) = \frac{U^*}{r^*\Omega^*}, \quad G(z) = \frac{V^*}{r^*\Omega^*}, \quad H(z) = \frac{W^*}{(\nu\Omega^*)^{\frac{1}{2}}}$$

  where $\mathbf{U} = \mathbf{U}^*(z)$ is the velocity profile in cylindrical polars, Ω^* is the rotation rate of the disk and ν is the kinematic viscosity.
- Worth noting - Reynolds number is equivalent to radial position on the disk.
- **Non-dimensional base flow**

$$\mathbf{U}^B = \left(\frac{r}{R}F, \frac{r}{R}G, \frac{1}{R}H\right)$$

Introduction to the Rotating Disk - Stability

- The disk admits an inviscid *crossflow* instability, similar to the one present in swept-wing flow, hence the analogy.

Introduction to the Rotating Disk - Stability

- The disk admits an inviscid *crossflow* instability, similar to the one present in swept-wing flow, hence the analogy.
- In 1995, Rebecca Lingwood discovered a local *absolute* instability in the rotating disk boundary layer - important because of its proximity to the experimentally observed critical Reynolds number for *transition* to turbulence.

Introduction to the Rotating Disk - Stability

- The disk admits an inviscid *crossflow* instability, similar to the one present in swept-wing flow, hence the analogy.
- In 1995, Rebecca Lingwood discovered a local *absolute* instability in the rotating disk boundary layer - important because of its proximity to the experimentally observed critical Reynolds number for *transition* to turbulence.
- This absolute instability is not present in the swept-wing configuration due to the lack of periodicity.

Introduction to the Rotating Disk - Stability

- The disk admits an inviscid *crossflow* instability, similar to the one present in swept-wing flow, hence the analogy.
- In 1995, Rebecca Lingwood discovered a local *absolute* instability in the rotating disk boundary layer - important because of its proximity to the experimentally observed critical Reynolds number for *transition* to turbulence.
- This absolute instability is not present in the swept-wing configuration due to the lack of periodicity.
- The disk flow is *globally* linearly stable, and even in strongly absolutely unstable regions, convective behaviour dominates eventually.

Understanding Stability

- *Local* behaviour can be analysed using standard techniques for solving the temporal or spatial Orr-Sommerfeld eigenvalue problem as discussed.

Understanding Stability

- *Local* behaviour can be analysed using standard techniques for solving the temporal or spatial Orr-Sommerfeld eigenvalue problem as discussed.
- *Global* behaviour can be analysed using direct numerical simulations (DNS).

Local Eigenvalue Problem

Usual Approach

- Derive perturbation equations in a similar fashion to the Orr-Sommerfeld problem.
- Reduce to a set of six first order ODEs which can be solved for the wavenumber α.

Local Eigenvalue Problem

Usual Approach

- Derive perturbation equations in a similar fashion to the Orr-Sommerfeld problem.
- Reduce to a set of six first order ODEs which can be solved for the wavenumber α.

Alternate Approach

- Solve a *velocity-vorticity formulation*, reducing perturbation equations to a set of three second order PDEs.

Local Eigenvalue Problem

Usual Approach

- Derive perturbation equations in a similar fashion to the Orr-Sommerfeld problem.
- Reduce to a set of six first order ODEs which can be solved for the wavenumber α.

Alternate Approach

- Solve a *velocity-vorticity formulation*, reducing perturbation equations to a set of three second order PDEs.

Normal mode approximation

$$\hat{\phi}(r,\theta,z,t) = \phi(z)e^{i(\alpha r+\beta R\theta-\omega t)}$$

Velocity-vorticity Formulation

$$\frac{\partial \xi_r}{\partial t} + \frac{1}{r}\frac{\partial N_r}{\partial \theta} - \frac{\partial N_\theta}{\partial z} - \frac{2}{R}\left(\xi_\theta + \frac{\partial w}{\partial r}\right) = \frac{1}{R}\left[\left(\nabla^2 - \frac{1}{r^2}\right)\xi_r - \frac{2}{r^2}\frac{\partial \xi_\theta}{\partial \theta}\right]$$

$$\frac{\partial \xi_\theta}{\partial t} + \frac{\partial N_r}{\partial z} - \frac{\partial N_z}{\partial r} + \frac{2}{R}\left(\xi_r - \frac{1}{r}\frac{\partial w}{\partial \theta}\right) = \frac{1}{R}\left[\left(\nabla^2 - \frac{1}{r^2}\right)\xi_\theta + \frac{2}{r^2}\frac{\partial \xi_r}{\partial \theta}\right]$$

$$\nabla^2 w = \frac{1}{r}\left(\frac{\partial \xi_r}{\partial \theta} - \frac{\partial (r\xi_\theta)}{\partial r}\right)$$

$$\mathbf{u} = (u_r, u_\theta, w), \quad \boldsymbol{\xi} = (\xi_r, \xi_\theta, \xi_z)$$

$$\mathbf{N} = (N_r, N_\theta, N_z) = (\nabla \times \mathbf{U}_B) \times \mathbf{u} + \boldsymbol{\xi} \times \mathbf{U}_B$$

$$u_r = -\int_z^\infty \left(\xi_\theta + \frac{\partial w}{\partial r}\right) dz, \quad u_\theta = \int_z^\infty \left(\xi_r - \frac{1}{r}\frac{\partial w}{\partial \theta}\right) dz$$

$$\xi_z = \frac{1}{r}\int_z^\infty \left(\frac{\partial (r\xi_r)}{\partial r} + \frac{\partial \xi_\theta}{\partial \theta}\right) dz$$

Local Eigenvalue Problem

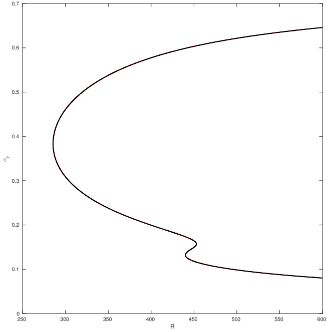

(a) Neutral Curve for α_r

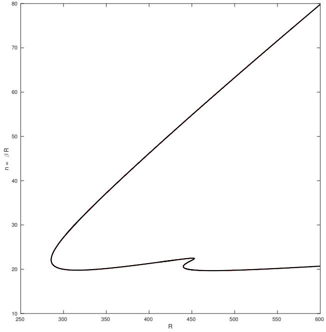

(b) Neutral Curve for $n = \beta R$

Global Behaviour

- Recall base flow profiles

$$\mathbf{U}^B = \left(\frac{r}{R} F, \frac{r}{R} G, \frac{1}{R} H \right)$$

Global Behaviour

- Recall base flow profiles

$$\mathbf{U}^B = \left(\frac{r}{R}F, \frac{r}{R}G, \frac{1}{R}H\right)$$

- *Parallel flow approximation* amounts to setting $r = R$.

Global Behaviour

- Recall base flow profiles

$$\mathbf{U}^B = \left(\frac{r}{R}F, \frac{r}{R}G, \frac{1}{R}H\right)$$

- *Parallel flow approximation* amounts to setting $r = R$.
- But base flow *varies with radius*, so this is not entirely physical.

Global Behaviour

- Recall base flow profiles

$$\mathbf{U}^B = \left(\frac{r}{R}F, \frac{r}{R}G, \frac{1}{R}H\right)$$

- *Parallel flow approximation* amounts to setting $r = R$.
- But base flow *varies with radius*, so this is not entirely physical.
- Small effect on local, eigenvalue analysis but major effect on global analysis when full temporal and radial variation incorporated.

Direct Numerical Simulations

Imagine an impulsive forcing to the disk surface at some radially localised location $r = r_e$.

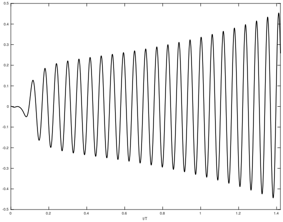

(a) Time history at $r = 540$

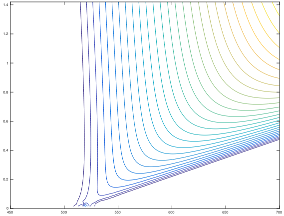

(b) Spatio-temporal development

Figure 3: Azimuthal mode number $n = 68$ and impulsive disturbance excited at $r = 520$ - homogeneous flow

Direct Numerical Simulations

Imagine an impulsive forcing to the disk surface at some radially localised location $r = r_e$.

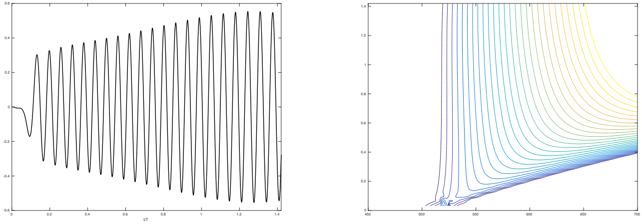

(a) Time history at $r = 540$ (b) Spatio-temporal development

Figure 4: Azimuthal mode number $n = 68$ and impulsive disturbance excited at $r = 520$ - inhomogeneous flow

Direct Numerical Simulations

Imagine an impulsive forcing to the disk surface at some radially localised location $r = r_e$.

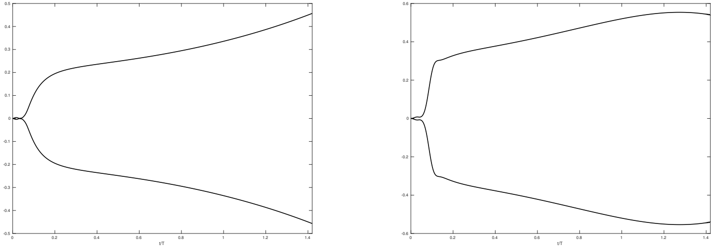

(a) Homogeneous (b) Inhomogeneous

Figure 5: Wavepacket envelopes at $r = 540$ azimuthal mode number $n = 68$ and an impulse excited at $r_e = 520$

Summary So Far

- Flow is *convectively* unstable for $R > 286$.

Summary So Far

- Flow is *convectively* unstable for $R > 286$.
- Flow has a *local absolute instability* which occurs for $R > 507$.

Summary So Far

- Flow is *convectively* unstable for $R > 286$.
- Flow has a *local absolute instability* which occurs for $R > 507$.
- Flow is *globally stable* when radial inhomogeneity is incorporated.

Periodic Modulation - Motivation

- We can adapt the steady problem to include a time-dependent part by way of oscillations of the disk.

Periodic Modulation - Motivation

- We can adapt the steady problem to include a time-dependent part by way of oscillations of the disk.
- Adding oscillations to **channel** flow can be stabilising.

Periodic Modulation - Motivation

- We can adapt the steady problem to include a time-dependent part by way of oscillations of the disk.
- Adding oscillations to **channel** flow can be stabilising.

$$u = \gamma_1 U_1^S + \gamma_2 U_2^P$$

where U_1^S and U_2^P are the steady base flow profiles for purely oscillatory channel flow ($\gamma_1 = 0$) and Poiseuille channel flow ($\gamma_2 = 0$).

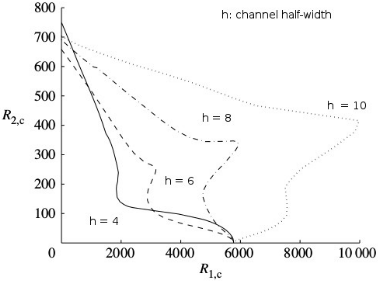

Periodic Modulation - Setup

- We can alter the von Kármán similarity variables to include a time-dependent structure

$$F(z, t) = \frac{U^*(z, t)}{r^* \Omega^*}, \quad G(z, t) = \frac{V^*(z, t)}{r^* \Omega^*}, \quad H(z, t) = \frac{W^*(z, t)}{(\nu \Omega^*)^{\frac{1}{2}}}$$

Periodic Modulation - Setup

- We can alter the von Kármán similarity variables to include a time-dependent structure

$$F(z,t) = \frac{U^*(z,t)}{r^*\Omega^*}, \quad G(z,t) = \frac{V^*(z,t)}{r^*\Omega^*}, \quad H(z,t) = \frac{W^*(z,t)}{(\nu\Omega^*)^{\frac{1}{2}}}$$

- System of ODEs becomes time-dependent

$$\begin{aligned} \frac{\partial F}{\partial t} &= F^2 - (G+1)^2 + F'H - F'' \\ \frac{\partial G}{\partial t} &= 2F(G+1) + G'H - G'' \\ H' &= -2F \end{aligned}$$

with

$$U(0,t) = W(0,t) = 0, \qquad V(0,t) = A\cos(\omega t)$$
$$U \to 0 \quad V \to -1 \quad \text{as} \quad z \to \infty$$

ROTATING FRAME

Periodic Modulation - Setup

- We can alter the von Kármán similarity variables to include a time-dependent structure

$$F(z,t)=\frac{U^*(z,t)}{r^*\Omega^*},\quad G(z,t)=\frac{V^*(z,t)}{r^*\Omega^*},\quad H(z,t)=\frac{W^*(z,t)}{(\nu\Omega^*)^{\frac{1}{2}}}$$

- System of ODEs becomes time-dependent

$$\frac{\partial F}{\partial t}=F^2-G^2+F'H-F''$$
$$\frac{\partial G}{\partial t}=2FG+G'H-G''$$
$$H'=-2F$$

with

$$U(0,t)=W(0,t)=0,\qquad V(0,t)=1+A\cos(\omega t)$$
$$U\to 0\qquad V\to 0\quad \text{as}\quad z\to\infty$$

NON-ROTATING (LAB) FRAME

Solution Method

- Map semi-infinite domain $[0, \infty)$ to computational domain $(0, 1]$ using mapping $\eta = \frac{l}{l+z}$

Solution Method

- Map semi-infinite domain $[0, \infty)$ to computational domain $(0, 1]$ using mapping $\eta = \frac{l}{l+z}$
- Express F and G in terms of odd Chebyshev series and H in terms of even ones:

$$\{F, G\}(\eta) \sim \sum_{n=1}^{\infty} a_n T_{2n-1}(\eta), \qquad H(\eta) \sim \frac{b_0}{2} + \sum_{n=1}^{\infty} b_n T_{2n}(\eta)$$

Solution Method

- Map semi-infinite domain $[0, \infty)$ to computational domain $(0, 1]$ using mapping $\eta = \frac{l}{l+z}$
- Express F and G in terms of odd Chebyshev series and H in terms of even ones:

$$\{F, G\}(\eta) \sim \sum_{n=1}^{\infty} a_n T_{2n-1}(\eta), \qquad H(\eta) \sim \frac{b_0}{2} + \sum_{n=1}^{\infty} b_n T_{2n}(\eta)$$

- Integrate equations twice with respect to η - e.g. for first equation

$$\iint \left(\frac{\partial F}{\partial t} + \mathcal{D}^2 F \right) = \iint \left(F^2 - G^2 - H\mathcal{D}F \right)$$

where $\mathcal{D} = \frac{d}{dz} = -\frac{\eta^2}{l} \frac{d}{d\eta}$ and similarly for $\mathcal{D}^2$

Solution Method

- Map semi-infinite domain $[0, \infty)$ to computational domain $(0, 1]$ using mapping $\eta = \frac{l}{l+z}$
- Express F and G in terms of odd Chebyshev series and H in terms of even ones:

$$\{F, G\}(\eta) \sim \sum_{n=1}^{\infty} a_n T_{2n-1}(\eta), \qquad H(\eta) \sim \frac{b_0}{2} + \sum_{n=1}^{\infty} b_n T_{2n}(\eta)$$

- Integrate equations twice with respect to η - e.g. for first equation

$$\iint \left(\frac{\partial F}{\partial t} + \mathcal{D}^2 F \right) = \iint \left(F^2 - G^2 - H\mathcal{D}F \right)$$

  where $\mathcal{D} = \frac{d}{dz} = -\frac{\eta^2}{l} \frac{d}{d\eta}$ and similarly for $\mathcal{D}^2$
- Matrix operators are pentadiagonal.

Solution Method

- Integrate equations twice with respect to η - e.g. for first equation

$$\iint \left(\frac{\partial F}{\partial t} + \mathcal{D}^2 F\right) = \iint \left(F^2 - G^2 - H\mathcal{D}F\right)$$

Solution Method

- Integrate equations twice with respect to η - e.g. for first equation

$$\iint \left(\frac{\partial F}{\partial t} + \mathcal{D}^2 F\right) = \iint \left(F^2 - G^2 - H\mathcal{D}F\right)$$

- Apply backward three-level scheme for time-discretisation

$$\left(\frac{\partial f}{\partial t}\right)_l = \frac{1}{2\Delta t}\left(3f_l - 4f_{l-1} + f_{l-2}\right)$$

Solution Method

- Integrate equations twice with respect to η - e.g. for first equation

$$\iint \left(\frac{\partial F}{\partial t} + \mathcal{D}^2 F \right) = \iint \left(F^2 - G^2 - H\mathcal{D}F \right)$$

- Apply backward three-level scheme for time-discretisation

$$\left(\frac{\partial f}{\partial t} \right)_l = \frac{1}{2\Delta t} \left(3f_l - 4f_{l-1} + f_{l-2} \right)$$

- Solve using predictor-corrector

$$\left(\frac{3}{2\Delta t} \iint + \iint \mathcal{D}^2 \right) F_{l+1} = \frac{2}{\Delta t} \iint F_l - \frac{1}{2\Delta t} \iint F_{l-1} + \iint \left(F_l^2 - G_l^2 - H_l \mathcal{D} F_l \right)$$

Solution Method

- Integrate equations twice with respect to η - e.g. for first equation

$$\iint \left(\frac{\partial F}{\partial t} + \mathcal{D}^2 F \right) = \iint \left(F^2 - G^2 - H \mathcal{D} F \right)$$

- Apply backward three-level scheme for time-discretisation

$$\left(\frac{\partial f}{\partial t} \right)_l = \frac{1}{2\Delta t} \left(3 f_l - 4 f_{l-1} + f_{l-2} \right)$$

- Solve using predictor-corrector

$$\left(\frac{3}{2\Delta t} \iint + \iint \mathcal{D}^2 \right) F_{l+1} = \frac{2}{\Delta t} \iint F_l - \frac{1}{2\Delta t} \iint F_{l-1} + \iint \left(F_l^2 - G_l^2 - H_l \mathcal{D} F_l \right)$$

- Oscillation is added after steady state is reached.

Preliminary Results

Imagine an impulsive forcing to the disk surface at some radially localised location $r = r_e$. Boundary conditions in the rotating frame are of the form $G(z=0) = \epsilon \cos(\omega t)$.

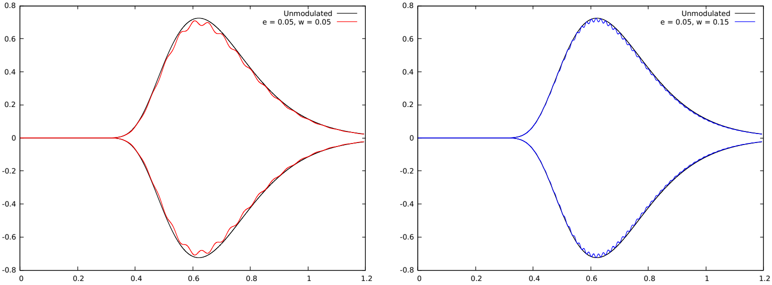

(a) $\epsilon = 0.05$ and $\omega = 0.05$

(b) $\epsilon = 0.05$ and $\omega = 0.15$

Figure 6: Wavepacket envelopes at $r = 450$ with azimuthal mode number $n = 28$ and an impulse excited at $r_e = 400$

Comparison with Garrett et. al. (2016) - Roughness

- Garrett et. al. (2016) use boundary conditions on G to approximate anisotropic roughness.
- They show that roughness component can be stabilising.
- Roughness component, *in some sense*, is similar to oscillatory motion.

Future Work

- Incorporate Floquet theory to further understand oscillatory component.

Future Work

- Incorporate Floquet theory to further understand oscillatory component.
- Quantify any apparent effects and provide a physical reasoning.

Future Work

- Incorporate Floquet theory to further understand oscillatory component.
- Quantify any apparent effects and provide a physical reasoning.
- Is an oscillatory component stabilising for the rotating disk?

Floquet Theory

- Take normal mode approximation of the form

$$p(r, \theta, z, t) = \hat{p}(z, t)e^{\mu\tau}e^{i(\alpha r + \beta R\theta)}$$

where $\hat{p}(z, t)$ is periodic in t and all of the exponential growth in time of p is factored into $e^{\mu t}$. Also $\tau = \omega t$ non-dimensionalises the time scale.

Floquet Theory

- Take normal mode approximation of the form

$$p(r, \theta, z, t) = \hat{p}(z, t) e^{\mu\tau} e^{i(\alpha r + \beta R \theta)}$$

  where $\hat{p}(z, t)$ is periodic in t and all of the exponential growth in time of p is factored into $e^{\mu t}$. Also $\tau = \omega t$ non-dimensionalises the time scale.

- Decompose time dependent base flow into

$$\mathbf{U}^B(z, t) = \mathbf{U}^{VK}(z) + \sum_{n=-\infty}^{\infty} u_n(z) e^{i\tau}$$

Floquet Theory

- Take normal mode approximation of the form

$$p(r,\theta,z,t) = \hat{p}(z,t)e^{\mu\tau}e^{i(\alpha r+\beta R\theta)}$$

  where $\hat{p}(z,t)$ is periodic in t and all of the exponential growth in time of p is factored into $e^{\mu t}$. Also $\tau = \omega t$ non-dimensionalises the time scale.

- Decompose time dependent base flow into

$$\mathbf{U}^{B}(z,t) = \mathbf{U}^{VK}(z) + \sum_{n=-\infty}^{\infty} u_n(z)e^{i\tau}$$

- Decompose $\hat{p}$ into harmonics such that

$$\hat{p} = \sum_{n=-\infty}^{\infty} \hat{p}_n(z)e^{in\tau}$$

  and substitute into equations.

Floquet Theory

- Take normal mode approximation of the form

$$p(r,\theta,z,t) = \hat{p}(z,t)e^{\mu\tau}e^{i(\alpha r+\beta R\theta)}$$

  where $\hat{p}(z,t)$ is periodic in t and all of the exponential growth in time of p is factored into $e^{\mu t}$. Also $\tau = \omega t$ non-dimensionalises the time scale.

- Decompose time dependent base flow into

$$\mathbf{U}^B(z,t) = \mathbf{U}^{VK}(z) + \sum_{n=-\infty}^{\infty} u_n(z)e^{i\tau}$$

- Decompose $\hat{p}$ into harmonics such that

$$\hat{p} = \sum_{n=-\infty}^{\infty} \hat{p}_n(z)e^{in\tau}$$

  and substitute into equations.

- Gives system of perturbation equations to solve for μ.